JOC The Journal of Organic Chemistry

ARTICLE

pubs.acs.org/joc

CO_2 Capture by Multivalent Amino-Functionalized Calix[4]arenes: Self-Assembly, Absorption, and QCM Detection Studies§

Laura Baldini, Monica Melegari, Valentina Bagnacani, Alessandro Casnati,* Enrico Dalcanale, Francesco Sansone, and Rocco Ungaro

Dipartimento di Chimica Organica e Industriale, Università di Parma, Parco Area delle Scienze 17/A, I-43124, Parma, Italy

Supporting Information

ABSTRACT: The reactivity of CO_2 with polyamino substrates based on calix[4]arenes and on a difunctional, noncyclic model has been studied. All the compounds react with CO_2 in chloroform to form ammonium carbamate salts. However, the number, topology, and conformational features of the amino-functionalized arms present on the multivalent scaffold have a remarkable influence on the reaction efficiency and on the product composition. Tetraaminocalix[4]arenes **1**−**3** rapidly and efficiently react with 2 equiv of CO_2, yielding highly stable hydrogen-bonded dimers formed by the self-assembly of two bis-ammonium bis-carbamate intramolecular salts. 1,3-Diaminocalix[4]arene **4** absorbs 1 mol of CO_2, affording less stable zwitterionic ammonium carbamates. Gemini compound **5** reacts with CO_2 in a 1:1 stoichiometry, forming hydrogen-bonded dimers of ammonium carbamate derivatives of moderate stability. For upper rim 1,3-diaminocalix[4]arene **6**, in addition to the labile intramolecular salt, the presence of a self-assembled polymer was also detected. These systems were fully characterized in solution by ^1H and ^{13}C NMR spectroscopy, whereas the corresponding gas−solid reactions were further investigated by QCM measurements. Interestingly, the high affinity and reversibility of CO_2 uptake shown by 1,3-diamino calix[4]arene **4** enabled us to attain a promising QCM device for carbon dioxide sensing.

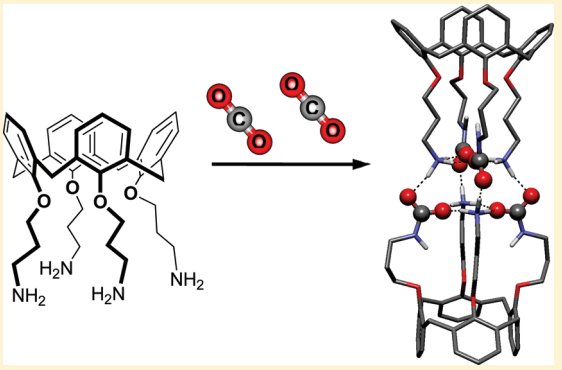

INTRODUCTION

The rapidly increasing level of carbon dioxide in the atmosphere is certainly one of the most urgent and limiting problems that the world will face in the next decades. It is, therefore, of great importance to develop systems able to trap and sequester CO_2 from the environment, processes that utilize CO_2 as a substrate or a reactant, and methods for efficient CO_2 monitoring.[1]

CO_2 is rather inert; nonetheless, it reacts rapidly and reversibly at ambient temperature and pressure with Lewis bases such as ammonia and primary or secondary amines in aqueous[2] and nonaqueous environments according to the equilibria in reactions 1 and 2

$$CO_2 + NHRR' \leftrightarrows RR'N - COOH \quad (1)$$

$$RR'N - COOH + NHRR' \leftrightarrows [RR'N - COO]^-[NH_2RR']^+ \quad (2)$$

Carbamic acids RR′N−COOH are usually thermally unstable and very difficult to isolate, because they either lose CO_2 or give the acid−base reaction 2 with a second equivalent of amine. Thus, the reaction of $CO_2(g)$ with an amine most often quantitatively yields the alkylammonium alkylcarbamate $[RR'N-COO]^-[NH_2RR']^+$ in which the two ions are held together by a salt bridge. This reactivity, which has been known for decades,[3] is currently receiving renewed popularity due to the present concern for CO_2 and is successfully being exploited in several systems and processes for the capture,[4,5] the use as a chemical feedstock,[6−10] and the sensing[11−14] of CO_2. Moreover, on account of the reversibility of reactions 1 and 2 and the propensity of the alkylammonium and alkylcarbamate ions to interact via electrostatic/hydrogen bonding interactions, the amine−CO_2 couple constitutes an appealing system also in the field of supramolecular chemistry, where it has been used to self-assemble various amine-containing building blocks to obtain, for example, lamellar materials,[15] thermally reversible organogels,[16,17] or a dynamic combinatorial library.[18] Interestingly, the use of polyamino substrates such as polyallylamine,[19] lysine peptides,[20] or amine-functionalized crown ethers[21] and calix[4]arenes[22−24] has led to the formation of supramolecular polymers with tailored properties. We were intrigued to note, however, that in all these systems based on polyamines no evidence of the occurrence of intramolecular ammonium−carbamate salt bridges had been reported, probably because either the reactions with CO_2 were conducted at high substrate concentration[19] or because the amino groups were linked to distant and divergent positions on the scaffold,[20−24] both cases favoring supramolecular polymerization. To the best of our knowledge, only in one case,[25] a

Received: December 13, 2010
Published: April 14, 2011

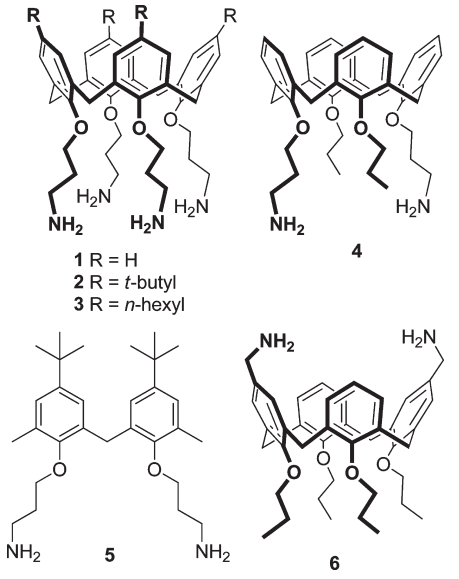

Figure 1. Structure of compounds **1**−**6**.

small diamine (a silylalkyldiamine) has been shown to absorb 1 mol of CO_2 per mole, and the formation of an intramolecular salt bridge in the zwitterionic carbamate was suggested. We conjectured that multiple amino groups preorganized in a convergent orientation could cooperate in reacting with CO_2, possibly forming intramolecular ammonium carbamate salts having enhanced stability and new properties. Calix[4]arenes provide a versatile platform for the multivalent presentation of reactive groups[26] because they have a variable number of reactive positions and well-defined conformational properties. We report herein the study of the reactivity with CO_2 of calix[4]arenes functionalized with multiple amino groups either at the upper or at the lower rim (**1**−**4** and **6**, Figure 1), and of a difunctionalized, noncyclic model (Gemini-type **5**, Figure 1). We found that these derivatives do indeed react with CO_2 in apolar solvents and in the solid state, forming intramolecular ammonium carbamate salts which, in some cases, self-assemble in hydrogen-bonded dimers. The ability of solid samples of some of these calixarenes to absorb CO_2 from the air was further investigated by QCM (quartz crystal microbalance) measurements. We show that 1,3-diaminocalix[4]arene **4**, because of its affinity and reversibility, can potentially be used as a CO_2 sensor.

RESULTS AND DISCUSSION

To investigate the reactivity of CO_2 with aminocalixarenes, we selected derivatives **1**−**6** having a different number and arrangement of amino groups. Calix[4]arenes **1**−**3** have four amines linked to the terminal carbon atom of a propyl chain at the calixarene lower rim and a different functionalization of the upper rim. The cone conformation of the scaffold ensures the spatial proximity of the four groups, while the propyl chains provide some conformational flexibility. 1,3-Diaminocalix[4]arenes **4** and **6** served to evaluate the effect of a lower number of animo groups and to examine the difference between lower and upper rim functionalization. Finally, the noncyclic Gemini **5** was chosen to study the role of the scaffold rigidity and preorganization. The reaction of amino derivatives **1**−**6** with CO_2 was performed by bubbling the gas through a solution of the amino compound in a deuterated solvent for 10 min, and the products were studied by ^{1}H and ^{13}C mono- and bidimensional NMR and IR spectroscopy.

***p*-H Tetraaminocalix[4]arene 1.** After CO_2 exposure, the ^{1}H NMR spectrum of tetraaminocalix[4]arene **1** in $CDCl_3$ appeared significantly changed (Figure 2) and revealed that the four amino groups of **1** had quantitatively reacted with two molecules of CO_2 to form two ammonium cations and two carbamate anions (compound **1a**, Scheme 1).

The NH carbamate signal emerged as a triplet at 4.74 ppm, while the NH_3^+ group resonates as a slightly broad signal at 9.35 ppm. Six signals (two of which are superimposed at 3.65 ppm) for the methylene groups of the two different alkyl chains of **1a** appeared instead of the three present in the spectrum of **1** and were fully assigned on the basis of a COSY experiment through the cross-peaks between the NH carbamate or the NH_3^+ protons and the respective α-methylene protons (inset, Figure 2). The simultaneous presence of alkylcarbamate and alkylammonium chains on the same calixarene molecule, in alternate positions at the lower rim, was proved by the existence of cross-peaks in the ^{1}H−^{1}H NOESY spectrum of **1a** between the N*H*CO and the β' and γ' protons and between the β' and α (or γ) protons (see Figure S18, Supporting Information). In the ^{13}C NMR spectrum, the signal of the carbamate carbon atom (C═O) appeared at 163.6 ppm, while free CO_2 was seen at 124.7 ppm. Moreover, every ^{13}C NMR signal of **1**, except for the $ArCH_2Ar$ methylene bridge, was replaced by a pair of 1:1 signals, due to the two different ammonium- and carbamate-terminating moieties. For example, the signal of the CH_2N carbon at 39.5 ppm in **1** was replaced by the peaks at 41.1 and 36.4 ppm due to the corresponding carbon atoms from the carbamate and ammonium ends, respectively. In the HMBC spectrum of **1a**, a cross-peak between the C═O carbon atom of the carbamate group and the α-methylene protons was observed (inset, Figure 2), which unambiguously proves the N−C carbamate bond formation. No precipitate was observed in the solution after CO_2 exposure, ruling out the formation of insoluble supramolecular polymers,[22,24] at least up to a calixarene concentration of 0.01 M.[27] The IR spectrum of the $CDCl_3$ solution of **1** after reaction with CO_2 showed a band at 1585 cm^{-1}, which could be assigned to the carbamate anion.[28]

Although the ^{1}H NMR spectrum of **1a** showed that the reaction between **1** and CO_2 takes place according to a 1:2 (**1**:CO_2) stoichiometry, no information about the actual structure of product **1a** could be obtained from these NMR data alone. Having two ammonium and two carbamate groups, in fact, **1a** could self-associate to form a hydrogen-bonded dimer, trimer, or (quite unlikely, because of the charged nature of the compound) a soluble oligomer which would give undistinguishable NMR spectra. The simultaneous presence of **1** and **1a** in one solution allowed us to measure their diffusion coefficients D (9.38×10^{-10} and 7.54×10^{-10} $m^2\ s^{-1}$ for **1** and **1a**, respectively) under the same conditions (i.e., the absolute temperature T and the viscosity of the solution η). On the basis of the Stokes−Einstein equation[29] $D = kT/(6\pi\eta r_H)$,[30] from the ratio of the D values, it was possible to directly determine the ratio of the hydrodynamic radii r_H of the two species. We found

$$r_H(\mathbf{1a})/r_H(1) = D(\mathbf{1})/D(\mathbf{1a}) = 1.25$$

Considering a spherical shape of the diffusing molecules,[31] this ratio indicates that the hydrodynamic volume (V_H) of **1a** is twice the V_H of **1**. We therefore conclude that in $CDCl_3$, at least in the concentration range 2×10^{-2} M to 2×10^{-4} M where no modifications of the ^{1}H NMR spectrum were observed, the product of the reaction of **1** with CO_2 is indeed a self-assembled dimer ($\mathbf{1a}_2$). The slightly broadened ^{1}H NMR signals of the

dx.doi.org/10.1021/jo200650f |*J. Org. Chem.* 2011, 76, 3720–3732

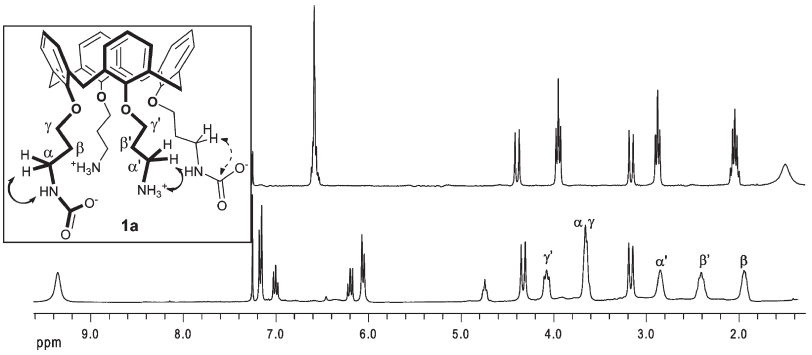

Figure 2. ^{1}H NMR spectra (300 MHz, $CDCl_3$, 298 K): (top) **1**; (bottom) **1** after saturation with CO_2. Inset: curved arrows = COSY cross-peaks; dashed curved arrow = HMBC cross-peaks.

Scheme 1. Reaction of 1−3 with CO_2(g) in $CDCl_3$

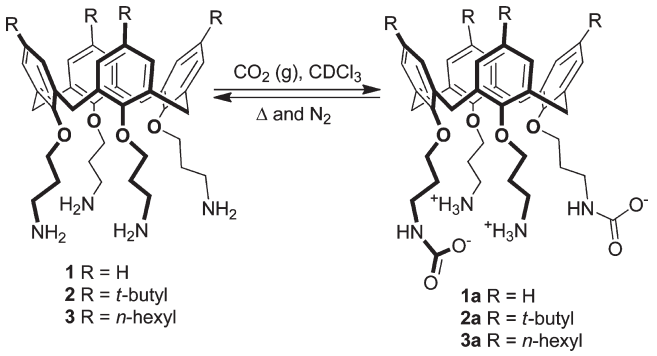

propylene protons suggest that the ammonium and carbamate groups are involved in noncovalent interactions that hinder the conformational freedom of the alkyl chains at the lower rim.

The ^{1}H NMR spectrum of $\mathbf{1a}_2$ also showed that the calixarene aromatic protons resonate in two groups separated by 1 ppm (Figure 2, bottom). This splitting can be produced by two causes: the influence of the two different substituents in proximal position at the calixarene lower rim, or a flattened cone conformation of the calixarene scaffold.[32,33] We found the latter to be the correct hypothesis, because in the ^{1}H NMR spectrum of the reaction product between the noncyclic compound **5** and CO_2 (**5a**, vide infra, Figure 7), the signals of the aromatic protons are nearly overlapping (Figure 7). Molecular modeling calculations taking into account NOESY and ROESY data yielded as the minimum energy conformer the structure reported in Figure 3. Two identical bis-ammonium bis-carbamate calixarenes form a hydrogen bonded dimer where all the CO and all the NH groups are involved in a seam of 12 hydrogen bonds, four of which are intermolecular and eight (four for each calixarene) intramolecular. The calixarenes adopt the flattened cone conformation with the aromatic rings linked to the carbamate-terminating chain pointing inward, and the carbamate NH groups are directed toward the interior of the molecule, as confirmed by the NOESY and ROESY cross-peaks between the NH and the β' and γ' methylene protons.

Interestingly, dimeric bis-ammonium bis-carbamate $\mathbf{1a}_2$ could also be obtained upon washing a dichloromethane or chloroform solution of **1** with a saturated aqueous solution of $NaHCO_3$. Treating the separated organic phase with anhydrous Na_2SO_4,

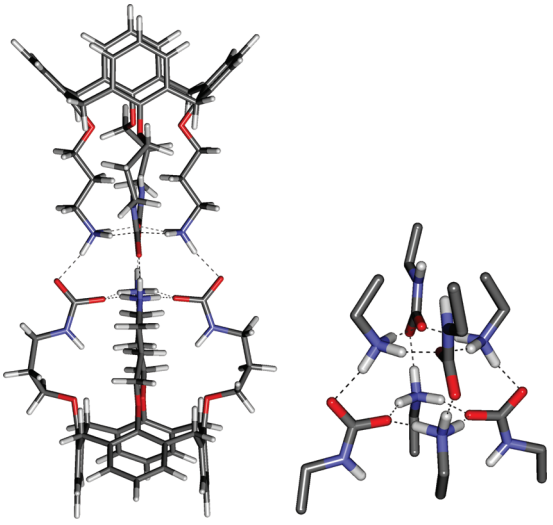

Figure 3. Energy-minimized structure of $\mathbf{1a}_2$ (left) and expansion of the hydrogen bonding motif (right, hydrogen atoms other than NH have been omitted for clarity).

evaporating the solvent, and drying the solid residue in vacuo did not affect the product composition. Moreover, spontaneous CO_2 absorption from the laboratory air was observed for **1** in the solid state. A sample of solid **1** was kept on the laboratory bench at room temperature, and portions were taken at subsequent time intervals, dissolved in $CDCl_3$, and subjected to NMR analysis. The ^{1}H NMR spectra (Figure 4) showed the presence of a mixture of free **1** and product $\mathbf{1a}_2$, with the amount of $\mathbf{1a}_2$ rapidly increasing (Figure 5). In particular, after 30 h, 50% of solid calix[4]arene **1** had reacted with CO_2.

These observations point to a remarkable affinity of **1** for CO_2, which is matched by a high stability of the dimeric bis-ammonium bis-carbamate $\mathbf{1a}_2$. The ^{1}H NMR spectra of $\mathbf{1a}_2$ stored at room temperature as solid or solution samples, in fact, remained unchanged for at least a few weeks, and no modifications were observed in the temperature range −45 to 50 °C. Moreover, in the NOESY and ROESY spectra of **1a**, at room temperature, no chemical exchange peaks were visible between the corresponding methylene protons of the ammonium- and carbamate-terminating alkyl chains. Together with the absence of coalescence of these signals up to 50 °C, these data mean that no exchange of the CO_2 molecule between the ammonium and carbamate part of

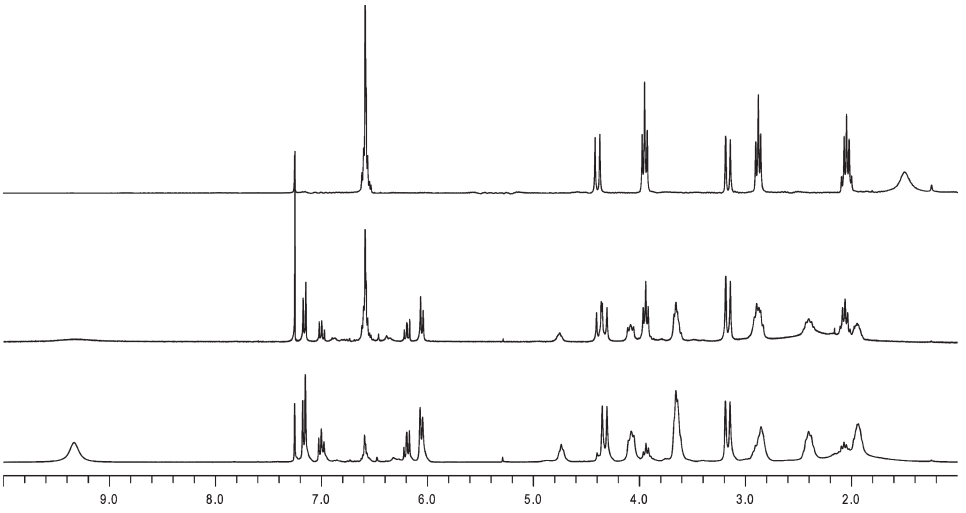

Figure 4. ^{1}H NMR spectra (300 MHz, $CDCl_3$, 298 K) of a solid sample of **1** stored on the laboratory bench taken at (top) t = 0, (middle) t = 45 h, (bottom) t = 27 days.

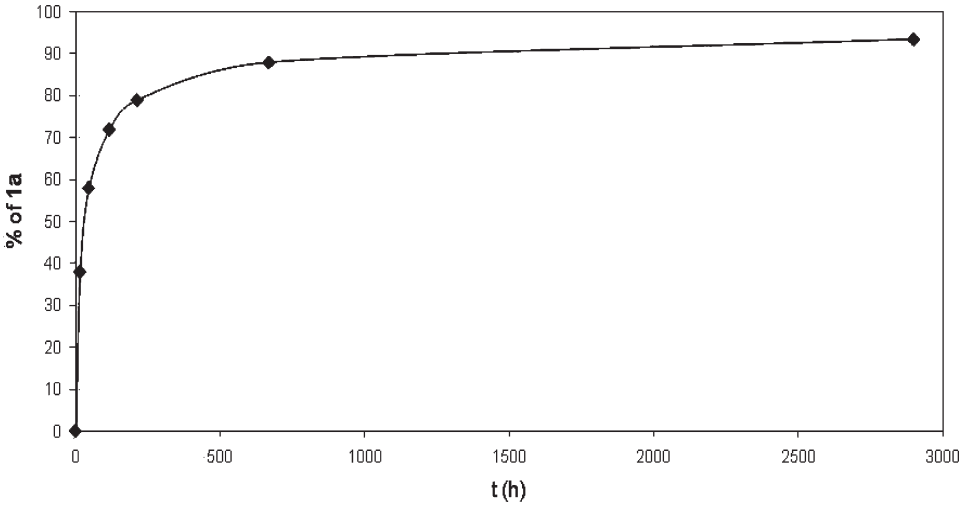

Figure 5. Kinetics of reaction of solid tetraamine **1** with atmospheric CO_2.

the molecule occurs, at least on the NMR time scale, as instead had been observed by George and Weiss for the alkylammonium alkylcarbamates obtained by reaction of n-decylamine with CO_2.[34]

The strength of the seam of 12 hydrogen bonds was studied by the addition of increasing amounts of CD_3OD to a 1×10^{-3} M solution of $\mathbf{1a_2}$ in $CDCl_3$. The dimer was perfectly stable up to the addition of 15% (v/v) of CD_3OD. Subsequent additions resulted in a decrease of the signals of $\mathbf{1a_2}$ and in the simultaneous appearance of a new set of resonances together with the signals of the free amine **1** (Figure S19 in Supporting Information). The new species diffuses with the same D as **1** (Figure S20 in Supporting Information) and can likely be attributed to a monomeric adduct of **1** with CO_2, which forms upon disruption of the intermolecular hydrogen bonds of $\mathbf{1a_2}$ by CD_3OD. The disappearance of the dimeric adduct $\mathbf{1a_2}$ is almost complete at $CDCl_3-CD_3OD$ 1:2.5 (v/v). The release of CO_2 from the adduct could also be achieved upon heating a solution of $\mathbf{1a_2}$ in $CDCl_3$ at 60 °C while flushing it with N_2. The ^{1}H NMR spectrum recorded after this treatment was identical to that of free **1**. Alternatively, the acidification of the solution of $\mathbf{1a_2}$ with HCl resulted in the disruption of the adduct and the formation of the tetraammonium cation of **1**.

The chemical inertness of $\mathbf{1a_2}$ was confirmed by adding allyl bromide and 18-crown-6 to its solution, to synthesize the corresponding allyl carbamate. As reported in a literature procedure,[6] the crown ether would form a "host−guest" complex with the alkylammonium cations, thus weakening their interactions with the carbamate anions, which, in turn, would be available to react as nucleophiles with allyl bromide. In our case, however, the ^{1}H NMR of the reaction mixture was the exact superposition of the spectra of the three components ($\mathbf{1a_2}$, 18-crown-6 and allyl bromide), indicating that the expected reaction did not take place and also that the crown ether did not significantly interact with the alkylammonium groups because of the strong hydrogen bonds.

In the polar, aprotic solvent DMSO-d_6, the reaction of **1** with CO_2 resulted in the quantitative formation of the tetracarbamic acid **1b** (Scheme 2). In the ^{1}H NMR spectrum, which shows that **1b** has maintained the C_4 symmetry of **1**, the NH proton

dx.doi.org/10.1021/jo200650f |J. Org. Chem. 2011, 76, 3720–3732

resonates at 6.76 ppm and the α methylene protons are shifted from 2.73 ppm for **1** to 3.12 ppm. In the ^{13}C NMR spectrum, the CO resonates at 157.5 ppm, and the α methylene carbon is shifted from 39.7 to 37.2 ppm. Free carbamic acids in DMSO or DMF solutions were observed spectroscopically for the first time by Rudkevich.[14,22] The rationale for their formation has been provided by a detailed study by Masuda et al.[28] on the role of the solvent in the reaction of CO_2 with amines. In fact, because the solvent has an influence on the acidity of the carbamic acid, i.e., the position of equilibrium in reaction 2, formation of either the carbamic acid or of the ammonium carbamate can be favored. Thus, bubbling CO_2 through a solution of the amine in highly polar aprotic solvents, such as DMSO, DMF, or pyridine results in the formation of the free carbamic acids because in these solvents the pK_a of the carbamic acid is higher than that of the ammonium salt. On the contrary, in apolar aprotic solvents such as benzene or chloroform, and in dipolar amphiprotic solvents such as 2-propanol or methanol, the same reaction produces the ammonium carbamates.

Scheme 2. Reaction of 1 with CO_2(g) in DMSO-d_6

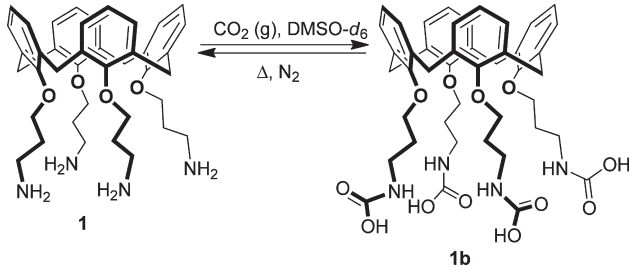

Scheme 3. Reaction of 4 with CO_2(g) in $CDCl_3$

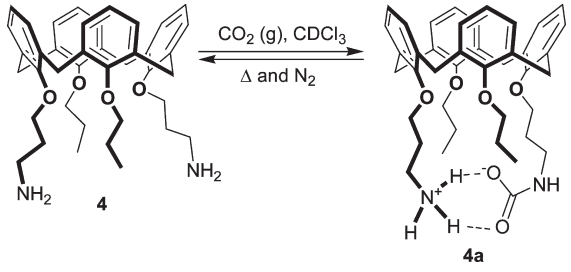

***p*-Alkyl Tetraaminocalix[4]arenes 2 and 3.** Also tetraamines **2** and **3**, substituted at the upper rim with four *tert*-butyl and four n-hexyl groups, respectively, react with CO_2(g) in $CDCl_3$, yielding the corresponding bis-ammonium bis-carbamate dimeric species $\mathbf{2a_2}$ and $\mathbf{3a_2}$ (Scheme 1). Interestingly, however, these compounds seemed to display an even increased affinity for CO_2 with respect to **1**. In fact, the ^1H NMR spectrum of **2** measured immediately after its synthesis showed, in addition to the resonances of the free amine **2**, the presence of a set of small peaks, corresponding to the CO_2 dimeric adduct $\mathbf{2a_2}$. Furthermore, the ^1H NMR of freshly synthesized **3** contained a ~1:1 ratio of the resonances of **3** and $\mathbf{3a_2}$. Evidently, the brief exposure of the CH_2Cl_2 solution of the aminocalixarenes **2** and **3** to the laboratory air during the reaction workup partially produced the carbamate salts. This had not been observed for **1** which, after the workup, was isolated in its free form.

***p*-H 1,3-Diaminocalix[4]arene 4.** The reaction of 1,3-diaminocalix[4]arene **4** with CO_2 in $CDCl_3$ produced a new species which, different from that of **1**−**3**, could be identified as a monomeric ammonium carbamate zwitterion (**4a**, Scheme 3). In the ^{13}C NMR spectrum of **4a** (Figure S22 in Supporting Information), the carbamate CO carbon resonates at 162.9 ppm, while the protons of the NH_3^+ and carbamate NH groups give broad signals at 6.24 ppm and 4.96 ppm, respectively, in the ^1H NMR spectrum (Figure S21 in Supporting Information). Moreover, the three CH_2 methylene signals of the $CH_2CH_2CH_2N$ chains in the ^1H NMR spectrum were replaced by six signals (two of which are superimposed at 4.10 ppm), belonging to the ammonium- and carbamate-terminating chains, which were fully assigned on the basis of COSY spectra. The $\Delta\delta$ between the aromatic protons of the phenol rings linked to the propyl and to the ammonium/carbamate-terminating chains is significantly increased with respect to the corresponding value in **4**, suggesting a flattened cone conformation of the calixarene scaffold. DOSY experiments carried out on a mixture of **4** and **4a** suggested a monomeric structure for **4a** ($D(\mathbf{4a}) = 5.45 \times 10^{-10}$ m^2 s^{-1}, $D(\mathbf{4}) = 5.58 \times 10^{-10}$ m^2 s^{-1}, $r_H(\mathbf{4a})/r_H(\mathbf{4}) = D(\mathbf{4})/D(\mathbf{4a}) = 1.03$). This implies the presence of an intramolecular salt bridge together with two hydrogen bonds between the diametral ammonium and carbamate

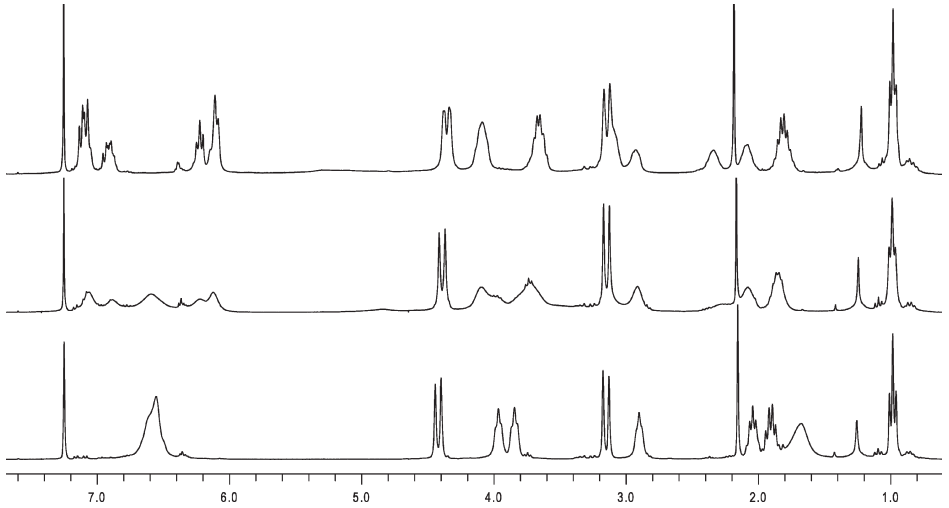

Figure 6. ^1H NMR spectra (300 MHz) of a $CDCl_3$ solution of **4** saturated with CO_2 at (top) −10 °C, (middle) 20 °C, and (bottom) 45 °C.

dx.doi.org/10.1021/jo200650f |*J. Org. Chem.* 2011, 76, 3720–3732

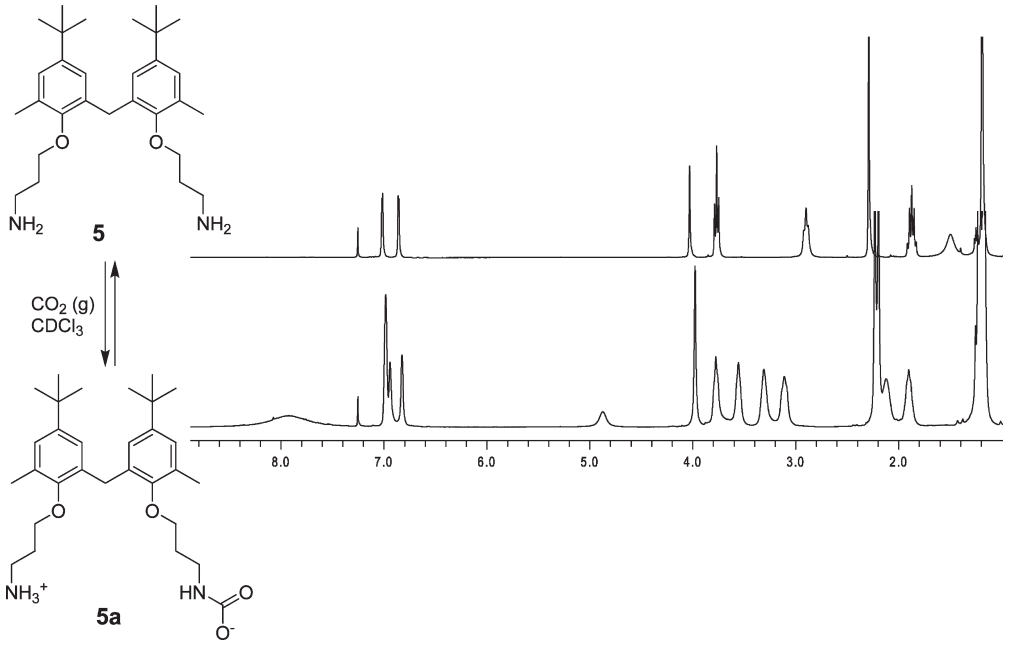

Figure 7. ^{1}H NMR spectra (300 MHz, $CDCl_3$, 298 K): (top) **5**; (bottom) **5** after saturation with CO_2.

groups. The ^{1}H NMR signals of the ammonium- and carbamate-terminating alkyl chains of **4a**, in fact, are broadened, indicating a restricted conformational freedom of these groups. Differently from tetraamino calixarenes **1**−**3**, the formation of a hydrogen-bonded dimer is disfavored by the presence of the propyl chains, which produces a sterical hindrance around the charged groups.

Similarly to **1**−**3**, solid **4** also reacts with CO_2, but in this case the reaction takes place only if **4** is exposed to pure CO_2, the CO_2 uptake from the air being insignificant on a time scale of a few days. The 1,3-diaminocalix[4]arene **4**, therefore, displays a decreased affinity for CO_2 compared to tetraamines **1**−**3**. Also the stability of **4a** in solution is significantly lower than the stability of **1a**−**3a**. A ^{1}H NMR spectrum registered a few days after the reaction of **4** with CO_2, in fact, showed the presence of the signals belonging both to **4a** and to free **4**, clear evidence that, in solution, CO_2 is slowly released from **4a**. Interestingly, a VT NMR study performed on the latter sample (Figure 6) showed that by increasing the temperature the amount of free **4** gradually increases (while **4a** decreases), until, at 45 °C, free **4** is the only species present in solution. On the contrary, by lowering the temperature, **4a** becomes the predominant species, until, at −10 °C, free **4** has totally disappeared. Apparently, **4** reacts again with the CO_2 dissolved in $CDCl_3$ solution. The process is reversible in both directions and for several cycles. This is a case where a small temperature variation shifts the balance between the enthalpic and entropic terms (both negative) in the free energy equation $\Delta G = \Delta H - T\Delta S$ for the equilibrium in reaction 3.

$$\mathbf{4} + CO_2 \leftrightarrows \mathbf{4a} \qquad (3)$$

Gemini 5. Model compound **5** can be considered as a "half calix[4]arene"; it has the same functional groups of **1** but lacks the macrocyclic connection. Bubbling CO_2 through a solution of **5** in $CDCl_3$ resulted in significant changes in the ^{1}H NMR spectrum, analogous to the ones observed for **1** and compatible with the conversion of the two amino groups into an alkylammonium and an alkylcarbamate functionality (Figure 7). Two broad signals appeared around 7.95 and at 4.88 ppm, assigned to the NH_3^+ and the carbamate NH protons, respectively. Six signals for the methylene protons of the ammonium- and carbamate-terminating alkyl chains substituted the three signals for the methylene groups of the propylamine chains of **6**. Two singlets were observed for the methyl Ar−CH_3 signals, two for the *tert*-butyl signals and four for the ArH protons, two of which are superimposed. In the ^{13}C spectrum, the C═O carbamate carbon atom resonates at 163.6 ppm.

Also in this case, the simultaneous presence of the two species allowed us to determine the ratio of their hydrodynamic radii by means of DOSY NMR (D(**5a**) = 1.17 × 10^{-9} m^2 s^{-1}, D(**5**) = 1.37 × 10^{-9} m^2 s^{-1}), which gave

$$r_H(\mathbf{5a})/r_H(\mathbf{5}) = D(\mathbf{5})/D(\mathbf{5a}) = 1.17$$

and

$$V_H(\mathbf{5a})/V_H(\mathbf{5}) = 1.6$$

On account of the nonspherical shape of **5**,[31] from this ratio we can hypothesize a dimeric structure for the product of the reaction of **5** with CO_2 (**5a$_2$**). The stability of the CO_2 dimeric adduct **5a$_2$** is significantly lower than the stability of **1a$_2$** and of **4a**. After storage of a solution of **5a$_2$** in a stoppered NMR tube for a few days, the spectrum revealed that CO_2 was slowly released and a mixture of **5a$_2$** and free **5** was present. The presence of monomeric ammonium carbamate zwitterions was not observed. Differently from **1a$_2$**, moreover, in the NOESY and ROESY spectra of **5a$_2$**, chemical exchange peaks are present between the α and α′, between the β and β', and between the γ and γ' methylene groups and between the two internal ArH protons, indicating that the CO_2 molecule is exchanging between the ammonium and the carbamate site.[34] Additionally, washing a chloroform solution of **5** with 0.1 M $NaHCO_3$ did not result in any modification of the ^{1}H NMR spectrum of **5** and no spontaneous absorption of CO_2 from the laboratory air was observed, neither for a solution of **5** nor for the compound in the

dx.doi.org/10.1021/jo200650f |*J. Org. Chem.* 2011, 76, 3720–3732

solid state. A structure compatible with the NOESY data and molecular modeling is reported in Figure 8. Two carbamate ammonium zwitterions are linked together by two intermolecular hydrogen bonds, which, together with the two intramolecular interactions, form a circular array of four equivalent hydrogen bonds.

We assume that the lower CO_2 absorption ability of Gemini compound **5** with respect to **1**−**3** and **4** is due to the reduced preorganization of the scaffold. Molecular modeling studies show that **5** in solution adopts a conformation having the two alkyl chains pointing to opposite directions (data not shown). The formation of $\mathbf{5a_2}$ requires a significant modification of the Gemini conformation that is compensated by the formation of the four strong hydrogen bonds, which occurs with no steric hindrance. Also in this case, moreover, we did not observe any evidence of polymer formation in the concentration range 0.2−80 mM.

Upper Rim 1,3-Diaminocalix[4]arene 6. Bubbling CO_2 (g) into a $CDCl_3$ solution of **6**, which is functionalized with two amino groups at the upper rim, resulted in small but relevant changes of the ^{1}H NMR spectrum that are not related to the modifications observed for compounds **1**−**5** and their CO_2 adducts. The spectrum of **6** (Figure 9, top) in $CDCl_3$ reflects an almost C_4 symmetry of the calixarene, which is the result of the fast interconversion between the two opposite flattened cone C_{2v} conformations: the one with the two substituted aromatic rings pointing outward, to minimize the steric repulsions (Scheme 4, left), and the one with the two substituted aromatic rings pointing inward as a consequence of a weak intramolecular hydrogen bond between the two NH_2 groups (Scheme 4, right).

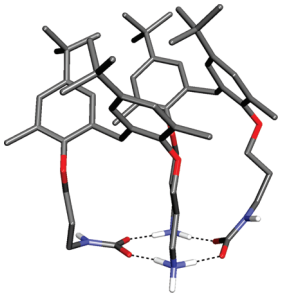

Figure 8. Energy-minimized structure of $\mathbf{5a_2}$. Hydrogen atoms other than NH have been omitted for clarity.

After reaction with CO_2 (Figure 9, bottom), the aromatic signals are split into two groups: a slightly broad doublet-triplet system, centered at 6.66 ppm, assigned to the aromatic protons of the unsubstituted rings and a singlet at 6.49 ppm, given by the aromatic protons of the para-substituted rings. The two triplets for the two different OCH_2 methylene groups at the lower rim are separated by 0.12 ppm, while in the ^{1}H NMR spectrum of **6** they are almost superimposed. The signal of the $ArCH_2N$ methylene group is broadened after the addition of CO_2. The NH_2 resonance at 1.54 ppm disappeared and a new broad signal appeared at 2.74 ppm. Moreover, some very broad signals appeared in the aromatic region and in the region between 2.50 and 4.50 ppm. This modification of the ^{1}H NMR spectrum is not as straightforward as the ones observed for the CO_2 adducts of compounds **1**−**5** having the amines at the lower rim. The separation of the aromatic signals in two groups and the increase in the chemical shift difference between the signals of the propyl chains at the lower rim, especially for the OCH_2 groups, indicate the predominance of the flattened cone conformation with the substituted aromatic rings pointing inward. As discussed above, such a conformation requires an attractive force that brings together the upper rim substituents. In our case, we attribute this intramolecular interaction to the formation of the ammonium−carbamate salt bridge in the adduct **6a** (Scheme 5).

The carbamate NH−CO bond, however, must be very labile, and the CO_2 must be exchanging fast between the two positions, because the signal of the $ArCH_2$ methylene group at the upper rim is not split into two signals ($ArCH_2NH_3^+$ and $ArCH_2NHCOO^-$), but only broadened. For the same reason, also the NH and NH_3^+ signals are not visible as distinct resonances. The very broad secondary signals, which are almost superimposed on the main signals, may indicate the presence of a supramolecular polymer held together by ammonium−carbamate salt bridges (**6b**, Scheme 5). The relative intensities of the broad peaks, in fact, slightly increase by increasing the concentration (in the range 1−100 mM). The

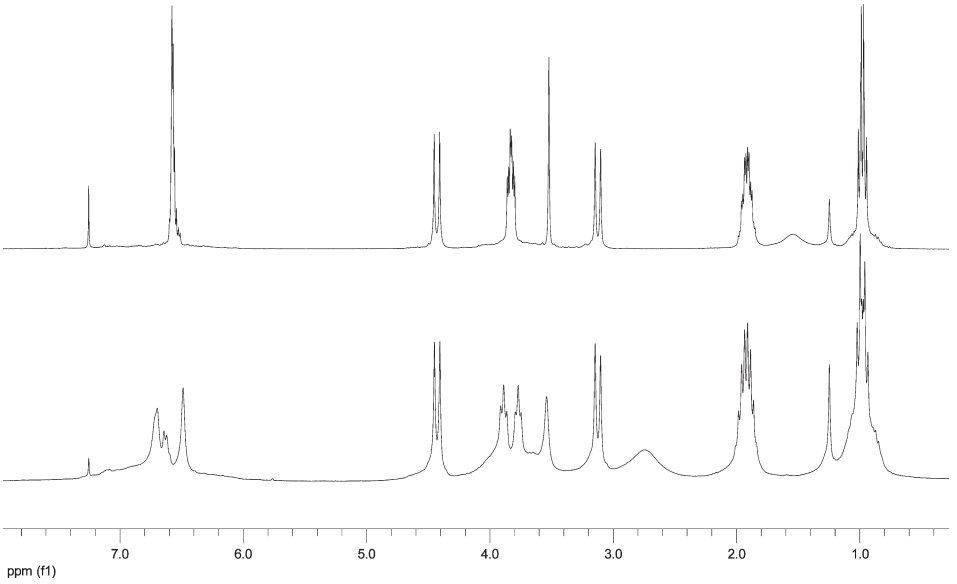

Figure 9. ^{1}H NMR spectra (300 MHz, $CDCl_3$, 298 K): (top) **6**; (bottom) **6** after saturation with CO_2; formation of **6a** + **6b**.

dx.doi.org/10.1021/jo200650f |J. Org. Chem. 2011, 76, 3720–3732

Scheme 4. Fast Interconversion of Two C_{2v} Flattened Cone Conformations of Compound 6

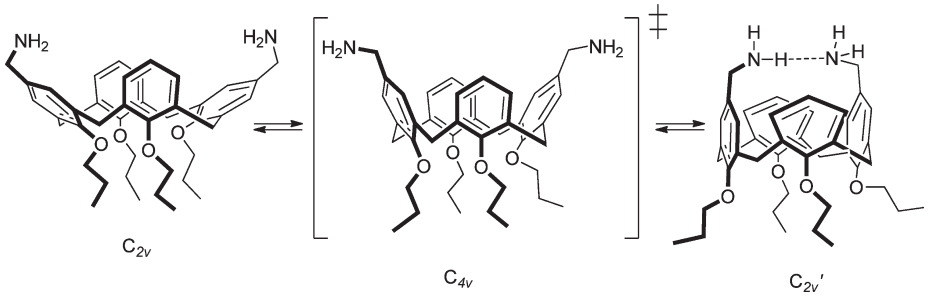

Scheme 5. Reaction of 6 with CO_2(g) in $CDCl_3$ and in DMSO-d_6

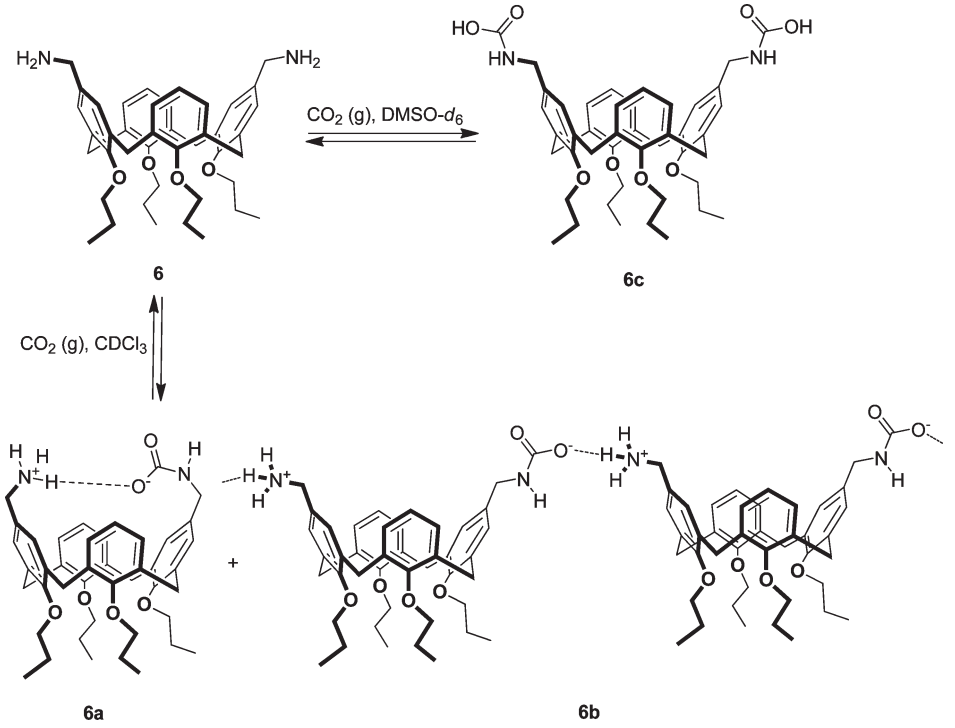

^{13}C NMR resonances are slightly broadened, and no signal for the carbamate CO is visible. Only the signal of free CO_2 is seen at 124.7 ppm. Both adducts **6a** and **6b**, however, are not very stable, because after a few days in the NMR tube the spectrum reversed back to that of the free amine **6**.

In DMSO-d_6, where the formation of intramolecular hydrogen bonds is disfavored, the spectrum of **6** (Figure 10, top) displays a C_{2v} symmetry and shows that the substituted aromatic rings are pointing outward (Scheme 4, left). Upon reaction with CO_2, a well-defined species is formed, compatible with the bis-carbamic acid (**6c**, Scheme 5). The carbamic acid NH protons (Figure 10, bottom) resonate as a broad triplet at 7.12 ppm, while the signal of the upper rim $ArCH_2N$ protons is shifted from 3.52 ppm to 4.02 and gives rise to a doublet (J = 5.7 Hz, typical of alkyl carbamic acids).[14] In the ^{13}C NMR spectrum, the CO carbon atom resonates at 157.0 ppm. This species is stable for several weeks in solution and is another example of the elusive carbamic acid.[14]

QCM Measurements. The spontaneous uptake of CO_2 by solid samples of calixarenes **1** and **4** prompted us to further investigate this gas−solid interaction by means of QCM measurements, with the ultimate goal of testing the feasibility of CO_2 sensors based on these compounds. Because the contributions of specific and nonspecific interactions could be dissected when comparing the QCM responses of different receptors,[35] we included in this study also Gemini **5**, tetrapropoxycalix[4]arene **7**, and monoamino-tripropoxycalix[4]arene **8** (Figure 11).

Compounds **1**, **4**, **5**, **7**, and **8** were deposited by spin coating on both sides of 10 MHz QCM transducers. The sensing capabilities of these coated QCMs toward CO_2 were thoroughly studied by exposing them to several fluxes of CO_2 at high (10^5 ppm) and low concentration ranges (10−20 ppm), and their responses were subsequently analyzed through Elovich kinetics isotherms.[36] The structural similarity of the four calixarenes allows a proper comparison of the sensor data, without any bias due to different solid-state packing and coating morphology, while the sensing capability of Gemini **5** can be related to that of diaminocalixarene **4** to evaluate the importance of the scaffold preorganization.

dx.doi.org/10.1021/jo200650f |*J. Org. Chem.* 2011, 76, 3720–3732

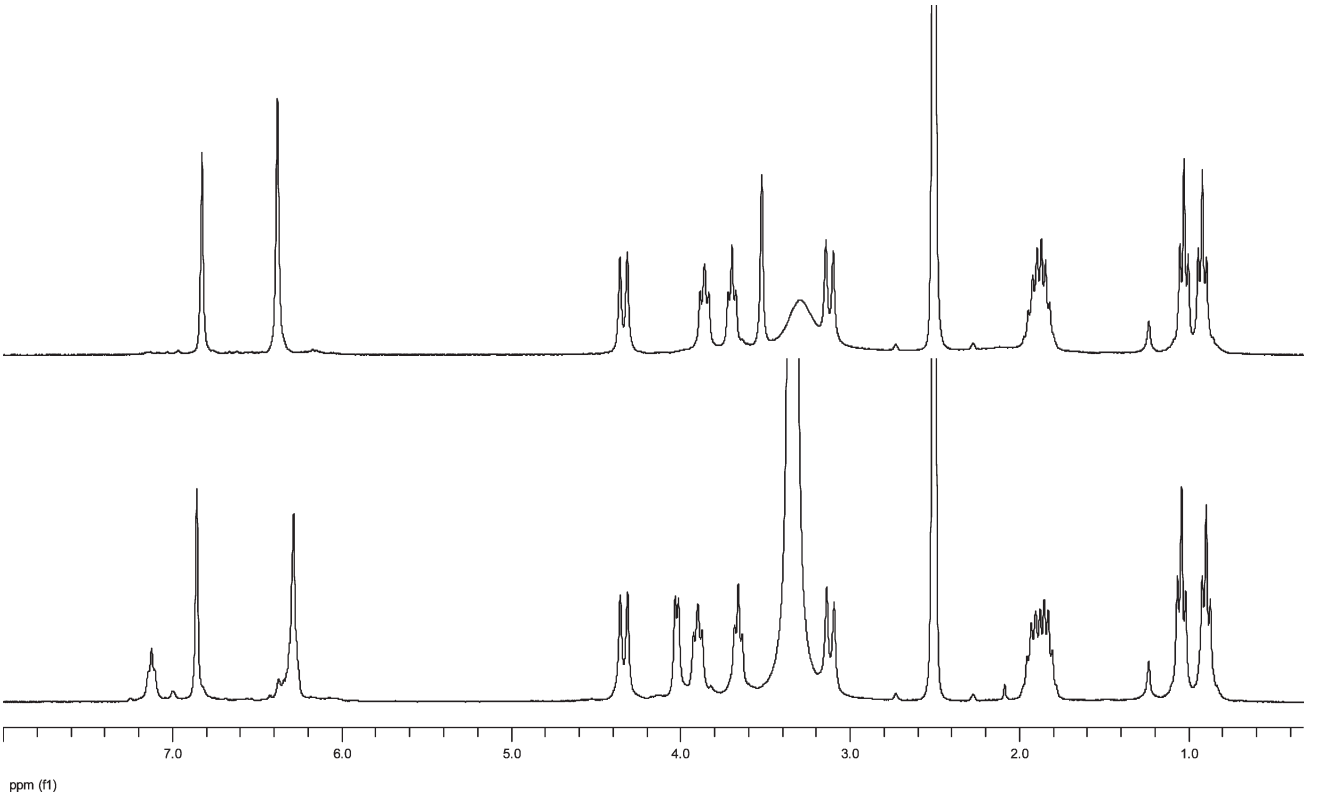

Figure 10. ^{1}H NMR spectra (300 MHz, DMSO-d_6, 298 K): (top) **6**; (bottom) **6** after saturation with CO_2; formation of **6c**.

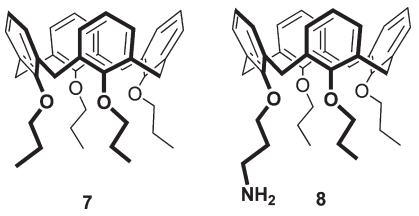

Figure 11. Structure of compounds **7** and **8**.

QCM responses (Δf) as a function of time (t) of the sensors coated with **1**, **4**, **5**, **7**, and **8** for CO_2 vapors at high concentration are shown in Figure 12. Tetraaminocalix[4]arene **1** (dark blue line) gives high but extremely slow responses, which are not reproducible and only partially reversible. In the first measurement, complete layer saturation is achieved and in the following responses a progressive loss of sensitivity is observed, indicating that this receptor is unsuitable for CO_2 sensing at the gas−solid interface. 1,3-Diaminocalix[4]arene **4**, on the other hand, proved a promising sensor for CO_2 detection; indeed, the red QCM trace shows the highest response, which is also reproducible and reversible. Interestingly, the response trace of Gemini **5** is similar in shape to the trace of **4**, but the Δf is smaller. Finally, the presence of only one (**8**, orange line) or no (**7**, green line) amino group on a calixarene scaffold drastically reduces or completely quenches the QCM responses.[37] Clearly, the proximity of two amino groups in compound **4**, which allows the formation of one intramolecular ammonium−carbamate interaction (**4a**), ensures at the same time the high response and the reversibility. Complete baseline recovery in the case of **4** is achieved upon fluxing with nitrogen for a long time or heating the sensor chamber by 10 °C.

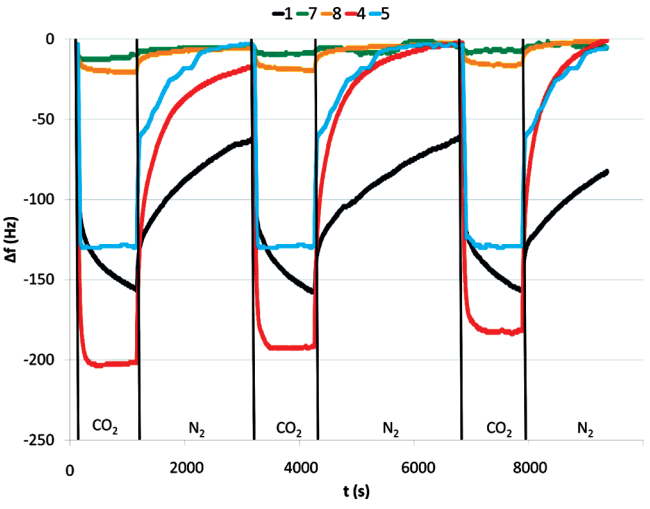

Figure 12. QCM response traces of compounds **1**, **4**, **5**, **7**, and **8** to CO_2 at 2×10^5 ppm.

The reduced response of conformationally mobile Gemini **5** (light blue line) confirms the fundamental role of the calixarene scaffold in preorganizing the amino groups, as observed in the solution studies. Instead, the 12 hydrogen bonding interactions of **1a** are thermodynamically too strong to be fully reversible, while the single amino group of **8** does not permit the formation of intramolecular ammonium−carbamate interactions leading to the layer inefficiency.

The responses of layers **4** and **8** to a low concentration flux of CO_2 are reported in Figure 13. The high difference in intensity

between the two layers is consistent with the previous results and confirms the good reproducibility and reversibility of the responses of **4** also outside the saturation range.

In order to further investigate the sorption process, the response phase (from the decrease due to the CO_2 flux to the plateau end) of the traces of layers **4** and **8**[38] were analyzed by Elovich kinetics.[39] According to this model, the surface covering Θ during the response phase is governed as a *function* of time by the following formula:[40]

$$\Theta(t) = \frac{1}{\beta}\ln(t) + K$$

where β and K are constants. This model is based on the assumption that the absorption probability of an analyte molecule during the analyte exposure (response phase) decreases exponentially as a function of the number of analyte molecules already adsorbed to the solid surface. Thus, by assuming that the resonant frequency (Δf) is related only to the interaction between CO_2 and the calixarene coatings, the value of Θ should be proportional to Δf. Hence, by plotting Δf as a function of $\ln(t)$, a linear relationship should be obtained. As can be observed from Figure 14, the trends of **4**- and **8**-coated QCMs are characterized by different behaviors. In particular, the calixarene **4** trace is approximately linear over the first 10 s and deviates from linearity at higher times. This indicates a chemisorption process, supporting a two-step interaction mode:[41] (i) a rapid, weak, and nonspecific interaction between the analyte molecules and the sensing layer and (ii) a slower but stronger specific interaction with the coating active sites. The linear region represents the fast process during which CO_2 molecules are adsorbed from the nonspecific sites of the calixarene coating, while the nonlinear region represents the slow CO_2 chemisorption due to the formation of the ammonium carbamate intramolecular salt. By contrast, the calix[4]arene **8**-coated QCM shows a completely linear behavior, indicating an interaction process totally dominated by nonspecific physisorption interactions.

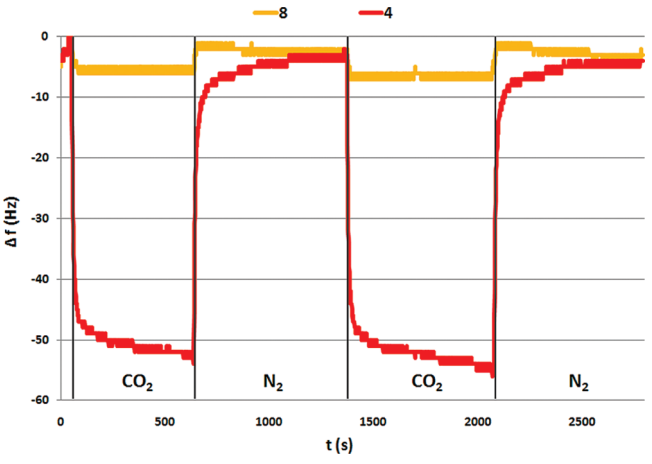

Figure 13. QCM responses traces of calix[4]arenes **8** and **4** to CO_2 at 20 ppm.

CONCLUSIONS

All the multivalent amino derivatives included in this study react with CO_2 in chloroform to form ammonium carbamate salts. The efficiency of CO_2 uptake and the composition and stability of the adducts, however, are strongly dependent on the number and the position of the amino groups and on the preorganization of the scaffold.

Tetraamino calix[4]arenes **1**−**3** absorb two molecules of CO_2 per calixarene, yielding self-assembled dimers where the eight charged groups of two bis-ammonium bis-carbamate calixarenes are interconnected by a seam of 12 intra- and intermolecular hydrogen bonds. This peculiar structure is responsible for the high stability of the adducts and for the remarkable efficiency of the reaction. Even in the solid state, in fact, **1**−**3** spontaneously absorb CO_2 from the air. Interestingly, among compounds **1**−**3**, the *p*-alkyl calixarenes **2** and **3** display an affinity for CO_2 higher than that of *p*-H calixarene **1**. As previously observed in calixarene chemistry,[42] the substitution pattern on the calixarene upper rim may have a strong influence on the function performed by the substituents at the lower rim. In this particular case, the increased efficiency in the CO_2 capture can be explained by a slight modification of the conformation of the *p*-alkyl calixarenes (two "less flattened" cone conformations rapidly interconverting) that favors the reaction with CO_2.

1,3-Diaminocalix[4]arene **4** forms with one molecule of CO_2 the intramolecular zwitterionic ammoniumcarbamate **4a**. Because of the lower number of hydrogen bonds/electrostatic interactions, **4a** is less stable but more labile than adducts $\mathbf{1a_2}$−$\mathbf{3a_2}$.

Gemini **5** and upper rim 1,3-diaminocalix[4]arene **6** display divergent orientation of the two amino groups. The reaction with CO_2 leads, also for these compounds, to the formation of the corresponding zwitterionic adducts, which, in the case of Gemini **5**, self-assemble in a hydrogen-bonded dimer. Because of the lack of preorganization, however, both **5** and **6** show a diminished

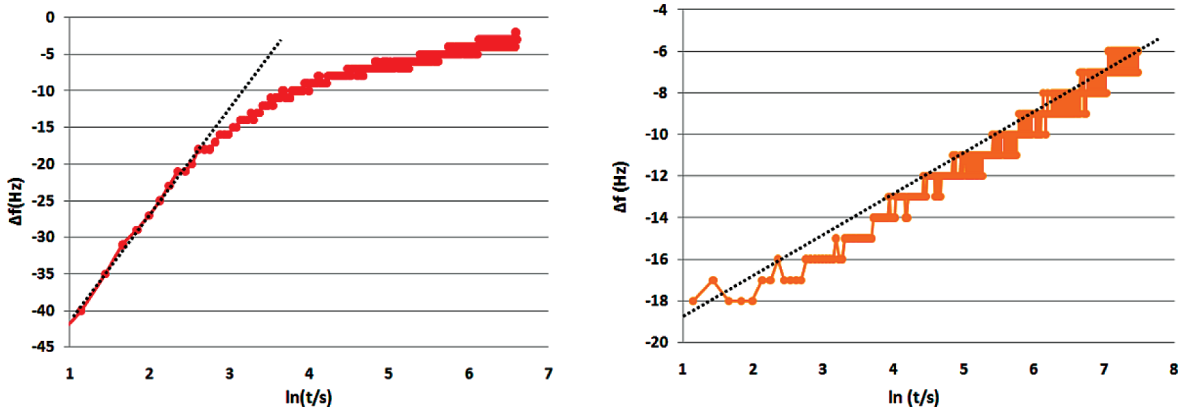

Figure 14. Elovich response kinetics for calix[4]arenes **4** (left) to 20 ppm and **8** (right) to 200 ppm of CO_2.

dx.doi.org/10.1021/jo200650f |*J. Org. Chem.* 2011, 76, 3720–3732

CO_2 affinity with respect to lower rim 1,3-diaminocalix[4]arene **4**. Moreover, in the case of calixarene **6**, a self-assembled polymer due to intermolecular ammonium−carbamate salt bridges was detected by ^{1}H NMR, together with the intramolecular adduct **6a**. This is the only evidence we obtained for polymer formation and can be attributed to conformational reasons: in the monomeric adduct **6a**, the interactions at the upper rim between the ammonium and the carbamate groups lead to a constrained, closed, flattened cone structure of the calixarene, while in polymer **6b**, the lower energy of the open, flattened cone conformation may be maintained.

Furthermore, we showed that 1,3-diaminocalix[4]arene **4** can be used as a sensing layer in QCM devices for the continuous monitoring of CO_2. The detection features of this sensor (fast response time, high sensitivity, and reversibility, and an operating temperature of 20 °C), in fact, are analogous or even superior to other polymer-based sensing layers.[43,44] Further studies aimed at assessing the detection limit, the influence of humidity, and the interference with other gases are currently underway.

Finally, a warning of general interest for chemists working with polyamino compounds: the correct storage of derivatives having multiple amino groups in close proximity is highly recommended in order to avoid undesired and sometimes hardly reversible reactions with atmospheric CO_2.

EXPERIMENTAL SECTION

General Experimental Methods. Tetraaminocalix[4]arenes **1**,[45] **2**,[46] and **3**,[47] upper rim 5,11-diaminocalix[4]arene **6**, [48] and tetrapropoxycalix[4]arene **7**[49] were synthesized according to literature procedures. 1,3-Diaminocalix[4]arene **4**, Gemini **5**, and monoaminocalix[4]arene **8** were synthesized in two steps, similarly to that for **1**−**3**, starting from 25,27-dipropoxycalix[4]arene,[50] 1,1-bis[(2-hydroxy-3-methyl-5-*tert*-butyl)phenyl]methane,[47] and 25,26,27-tripropoxycalix[4]arene,[51] respectively (see reaction Schemes S1 and S2 in Supporting Information). When reported, the peak assignments are made on the basis of atom connectivities determined by ^{1}H−^{1}H COSY, ^{1}H−^{1}H NOESY, and ^{1}H−^{13}C HMQC spectra.

General Procedure for the Alkylation of 25,27-Dipropoxy- and 25,26,27-Tripropoxycalix[4]arene and of Bis[(2-hydroxy-3-methyl-5-*tert*-butyl)phenyl]methane with *N*-(3-Bromoalkyl)phthalimide (synthesis of compounds 9−11). A suspension of the appropriate phenol compound (4.70 mmol) and NaH (60 wt.% in oil, 2.3 equiv per OH group) in dry DMF (80 mL) was stirred for 30 min, and then *N*-(3-bromoalkyl)phthalimide (2.3 equiv per OH group) was added. The reaction was monitored by TLC (eluent: hexane/ethyl acetate 8:2 (v/v)) and, when complete (3 h−1 day, depending on the substrate), was quenched by adding 1 N HCl (70 mL). The resulting solid was filtered through a Büchner funnel.

25,27-Bis(3-phthalimidopropoxy)-26,28-dipropoxycalix[4]arene (9). The crude product was purified by recrystallization in CH_2Cl_2/CH_3OH and obtained as a white solid. Yield 1.04 g (25%). Mp 132−134 °C. ^{1}H NMR (300 MHz, $CDCl_3$): δ 7.84−7.80 (m, 4H, Pht), 7.72−7.68 (m, 4H, Pht), 6.76 (d, J = 6.5 Hz, 4H, ArH), 6.67 (m, 2H, ArH), 6.43 (s, 6H, ArH), 4.42 (d, J = 13.4 Hz, 4H, H_{ax} of ArCH_2Ar), 4.08 (t, J = 7.3 Hz, 4H, O$CH_2$$CH_2$$CH_2$N), 3.87 (t, J = 7.3, 4H, OCH$_2$CH$_2$$CH_2$N), 3.77 (t, J = 7.3 Hz, 4H, O$CH_2$$CH_2$$CH_3$), 3.15 (d, J = 13.4 Hz, 4H, H_{eq} of ArCH_2Ar), 2.34 (quint, J = 7.3 Hz, 4H, OCH$_2$$CH_2CH_2$N), 1.85 (sext, J = 7.3 Hz, 4H, OCH$_2$$CH_2$$CH_3$), 0.93 (t, J = 7.3 Hz, 6H, OCH$_2$CH$_2$$CH_3$). ^{13}C NMR (75 MHz, $CDCl_3$): 168.1 (CO), 156.7 and 155.9 (Ar_{ipso}), 135.7 and 134.3 (Ar_{ortho}), 133.8 (Pht), 132.2 (Pht), 128.4 and 127.8 (Ar_{meta}), 123.1 (Ar), 122.2 and 121.9 (Ar_{para}), 76.9 (O$CH_2$$CH_2$$CH_3$), 72.4 (O$CH_2$$CH_2$$CH_2$N), 35.4 (OCH$_2CH_2$$CH_2$N), 31.0 (Ar$CH_2$Ar), 29.6 (OCH$_2$$CH_2$$CH_2$N), 23.3 (OCH$_2$$CH_2$$CH_3$), 10.5 (OCH$_2$$CH_2$$CH_3$). MS (ESI): m/z 905.5 (100%) $[M + Na]^+$. Anal. Calcd for $C_{56}H_{54}N_2O_8$: C, 76.17; H, 6.16; N, 3.17. Found: C, 76.30; H, 5.88; N, 3.11.

Bis{[2-(3-phthalimidopropoxy)-5-*tert*-butyl-3-methyl]-phenyl}methane (10). The crude product was purified by flash column chromatography (eluent: CH_2Cl_2) and obtained as a white foam. Yield 1.51 g (45%). Mp 62−63 °C. ^{1}H NMR (300 MHz, $CDCl_3$) δ 7.83−7.78 (m, 4H, Pht), 7.71−7.65 (m, 4H, Pht), 6.98 (d, J = 2.4 Hz, 2H, ArH), 6.83 (d, J = 2.4 Hz, 2H, ArH), 4.01 (s, 2H, ArCH_2Ar), 3.87 (t, J = 6.5 Hz, 4H, OCH_2), 3.78 (t, J = 6.3 Hz, 4H, OCH$_2$CH$_2$$CH_2$), 2.27 (s, 6H, Ar$CH_3$), 2.14 (quint, J = 7.7 Hz, 4H, OCH$_2$$CH_2$), 1.18 (s, 18H, *t*Bu). ^{13}C NMR (75 MHz, $CDCl_3$) δ 168.2, 153.4, 146.0, 133.7, 132.8, 132.1, 129.7, 125.8, 125.5, 123.1, 70.1, 35.6, 34.0, 31.3, 29.5, 29.4, 16.7. MS (ESI): m/z 737.5 (100%) $[M + Na]^+$. Anal. Calcd for $C_{45}H_{50}N_2O_6$: C, 75.50; H, 7.05; N, 3.92. Found: C, 75.32; H, 7.34; N, 3.85.

25-(3-Phthalimidopropoxy)-26,27,28-tripropoxycalix-[4]arene (11). The crude was purified by flash column chromatography (eluent: hexane/ethyl acetate 93:7 (v/v)) and obtained as a white solid. Yield 2.43 g (70%). Mp 63−65 °C. ^{1}H NMR (300 MHz, $CDCl_3$): δ 7.88−7.85 (m, 2H, Pht), 7.74−7.71 (m, 2H, Pht), 6.69−6.63 (m, 6H, ArH), 6.53−6.50 (m, 6H, ArH), 4.46 (d, 2H, J = 13.2 Hz, H_{ax} of ArCH_2Ar), 4.43 (d, 2H, J = 13.2 Hz, H_{ax} of ArCH_2Ar), 4.03 (t, 2H, J = 7.1 Hz, OCH_2CH$_2$CH$_2$N), 3.89 (t, 2H, J = 7.1 Hz, OCH$_2$CH$_2$$CH_2$N), 3.89−3.80 (m, 6H, O$CH_2CH_2$$CH_3$), 3.17 (d, 2H, J = 13.2 Hz, H_{eq} of ArCH_2Ar), 3.15 (d, 2H, J = 13.2 Hz, H_{eq} of ArCH_2Ar), 2.34 (quint, 2H, J = 7.1 Hz, OCH$_2$$CH_2CH_2$N), 1.95−1.86 (m, 6H, OCH$_2$$CH_2$$CH_3$), 0.99 (t, 6H, J = 7.5 Hz, OCH$_2$CH$_2$$CH_3$), 0.96 (t, 3H, J = 7.5 Hz, OCH$_2$CH$_2$$CH_3$). ^{13}C NMR (75 MHz, $CDCl_3$): 168.1, 156.7, 156.4, 156.2, 135.4, 134.7, 134.6, 133.8, 132.1, 128.3, 128.1, 128.0, 127.9, 123.1, 122.1, 121.8, 76.8, 76.5, 72.3, 35.4, 31.0, 30.9, 29.5, 23.3, 23.1, 10.4, 10.2. MS (ESI): m/z 760.4 (100%) $[M + Na]^+$. Anal. Calcd for $C_{48}H_{51}NO_6$: C, 78.13; H, 6.97; N, 1.90. Found: C, 77.95; H, 6.74; N, 2.14.

General Procedure for the Removal of the Phthaloyl Protecting Groups. A solution of calix[4]arenes **9** or **11** or Gemini **10** (1.70 mmol) and hydrazine monohydrate (50 equiv per phthalimide group) in ethanol (50 mL) was refluxed overnight. The solvent was then removed under reduced pressure, and the residue was dissolved in CH_2Cl_2 (50 mL) and water (40 mL). The organic phase was separated, and the water phase was extracted with CH_2Cl_2 (3 × 40 mL). The combined organic layers were dried over anhydrous Na_2SO_4, and the pure compounds were obtained after evaporation of the solvent under reduced pressure.

25,27-Bis(3-aminopropoxy)-26,28-dipropoxycalix[4]arene (4). White solid. Yield 0.98 g (93%). Mp 124−126 °C. ^{1}H NMR (300 MHz, $CDCl_3$): δ 6.79−6.38 (m, 6H, ArH), 6.52 (s, 6H, ArH), 4.43 (d, 4H, J = 13.3 Hz, H_{ax} of ArCH_2Ar), 3.94 (t, 4H, J = 7.1 Hz, OCH_2CH$_2$CH$_2$NH$_2$), 3.86 (t, 4H, J = 7.4 Hz, OCH_2CH$_2$$CH_3$), 3.16 (d, 4H, J = 13.3 Hz, H_{eq} of ArCH_2Ar), 2.90 (t, 4H, J = 6.9 Hz, OCH$_2$CH$_2$$CH_2NH_2$), 2.04 (quint, 4H, J = 7.0 Hz, OCH$_2$$CH_2CH_2NH_2$), 1.92 (sext, 4H, J = 7.4 Hz, OCH$_2$$CH_2$$CH_3$), 0.98 (t, 6H, J = 7.4 Hz, OCH$_2$CH$_2$$CH_3$). ^{13}C NMR (75 MHz, CD_3OD): 158.3 and 157.1 (Ar_{ipso}), 137.0 and 135.5 (Ar_{ortho}), 129.6 and 129.1 (Ar_{meta}), 123.1 and 123.0 (Ar_{para}), 77.8 (OCH$_2$CH$_2$$CH_3$), 73.9 (O$CH_2CH_2CH_2NH_2$), 40.0 (OCH$_2CH_2CH_2NH_2$), 34.5 (OCH$_2CH_2CH_2NH_2$), 31.9 (Ar$CH_2$Ar), 24.4 (OCH$_2CH_2$$CH_3$), 10.7 (OCH$_2CH_2$$CH_3$). MS (ESI): m/z 623.5 (100%) $[M + H]^+$. Anal. Calcd for $C_{40}H_{50}N_2O_4$: C, 77.14; H, 8.09; N, 4.50. Found: C, 76.98; H, 8.30; N, 4.78.

Bis[2-(3-aminopropoxy)-5-*tert*-butyl-3-methylphenyl]-methane (5). Colorless oil. Yield 0.73 g (95%). ^{1}H NMR (300 MHz, $CDCl_3$) δ 7.02 (d, 2H, J = 2.4 Hz, ArH), 6.86 (d, 2H, J = 2.4 Hz, ArH), 4.04 (s, 2H, ArCH_2Ar), 3.77 (t, J = 6.2 Hz, 4H, OCH_2), 2.90 (t, J = 6.8 Hz, 4H, OCH$_2$CH$_2$$CH_2$), 2.30 (s, 6H, Ar$CH_3$), 1.88 (quint, J = 6.5 Hz, 4H, OCH$_2$$CH_2$), 1.50 (bs, 4H, NH_2), 1.20 (s, 18H, *t*Bu). ^{13}C NMR

(75 MHz, $CDCl_3$) δ 153.5, 146.0, 132.8, 129.8, 125.8, 125.5, 70.6, 39.5, 34.2, 34.1, 31.3, 29.6, 16.6. MS (ESI): m/z 477.4 (100%) $[M + Na]^+$. Anal. Calcd for $C_{29}H_{46}N_2O_2$: C, 76.60; H, 10.20; N, 6.16. Found: C, 76.72; H, 9.95; N, 6.11.

25-(3-Aminopropoxy)-26,27,28-tripropoxycalix[4]arene (8). White solid. Yield 0.93 g (90%). Mp 178−179 °C. ^{1}H NMR (300 MHz, $CDCl_3$): δ 6.68−6.59 (m, 6H, ArH), 6.56−6.55 (m, 6H, ArH), 4.47 (d, 2H, J = 13.3 Hz, H_{ax} of ArCH_2Ar), 4.45 (d, 2H, J = 13.3 Hz, H_{ax} of ArCH_2Ar), 3.97 (t, 2H, J = 7.1 Hz, O$CH_2$$CH_2$$CH_2$$NH_2$), 3.88 (t, 4H, J = 7.8 Hz, O$CH_2$$CH_2$$CH_3$), 3.85 (t, 2H, J = 8.8 Hz, O$CH_2$$CH_2$$CH_3$), 3.17 (d, 2H, J = 13.3 Hz, H_{eq} of ArCH_2Ar), 3.16 (d, 2H, J = 13.3 Hz, H_{eq} of ArCH_2Ar), 2.91 (t, 4H, J = 7.1 Hz, OCH$_2$CH$_2$CH_2NH$_2$), 2.07 (quint, 2H, J = 7.1 Hz, OCH$_2$CH_2CH$_2$NH$_2$), 1.95−1.90 (m, 6H, OCH$_2$CH_2CH$_3$), 1.02 (t, 3H, J = 7.4 Hz, OCH$_2$CH$_2$CH_3), 1.00 (t, 6H, J = 7.4 Hz, OCH$_2$CH$_2$CH_3). ^{13}C NMR (75 MHz, $CDCl_3$): 156.6, 156.3, and 156.2 (Ar_{ipso}), 135.3, 135.1, 134.9, and 134.8 (Ar_{ortho}), 128.2, 128.1, 128.0, and 127.9 (Ar_{meta}), 122.0 and 121.8 (Ar_{para}), 76.6 (OCH$_2$CH$_2$CH$_3$), 72.6 (OCH$_2$CH$_2$CH$_2$NH$_2$), 39.4 (OCH$_2$CH$_2$CH$_2$NH$_2$), 34.3 (OCH$_2$-CH$_2$CH$_2$NH$_2$), 30.9 (ArCH$_2$Ar), 23.2 (OCH$_2$CH$_2$CH$_3$), 10.4 and 10.3 (OCH$_2$CH$_2$CH$_3$). MS (ESI): m/z 608.4 (100%) $[M + H]^+$. Anal. Calcd for $C_{40}H_{49}NO_4$: C, 79.04; H, 8.13; N, 2.30. Found: C, 79.35; H, 8.29; N, 2.03.

General Procedure for the Reaction of Amines with CO_2. CO_2(g) was bubbled with a needle through a solution of the amine (∼0.1−100 mM) in the deuterated solvent in the NMR tube for 7−10 min. After the bubbling, the NMR spectra were measured.

Molecular Modeling. Molecular modeling was carried out at the molecular mechanics (MMFF94 force field) and semiempirical (AM1) level by a combination of geometry optimization and conformational search (Monte Carlo) using the program SPARTAN 10.[52]

QCM Apparatus. Sensing measurements were performed using AT-cut quartz with a fundamental frequency of 10 MHz and a crystal diameter of 8 mm. Thin films of the amino derivatives were deposited by spin coating on both sides of the quartz transducers. QCM sensors are mass transducers where the frequency of oscillation, for small increases of mass, is governed linearly by the Sauerbrey equation:[53]

$$\Delta f = k\Delta m$$

where the Δf is the frequency variation of a Δm increase of mass. The quartz constant is experimentally estimated to be $k_q = -0.46$ Hz ng^{-1}: this value provides a nominal mass resolution of 1.6 ng Hz^{-1},[54] considering a minimum reliable frequency measurement of 1 Hz. In order to control the amount of the deposited films, QCM frequency was monitored online during the deposition process by a high stability frequency counter. A total frequency variation of $\Delta f = -20 \pm 0.5$ kHz was obtained for all samples produced.

The measurement system (Gaslab 20.1; IFAK, Magdeburg) is equipped with a flow chamber, containing four coated quartz crystals, a reference quartz crystal, and a thermocouple. The chamber was thermostatted at 20 ± 0.1 °C. The QCM chamber is connected with two mass-flow controllers (Brooks 5850S): one allows control over the flow rate of carbon dioxide mixture from 2 to 50 mL/min, and the other controls the flow rate of pure nitrogen from 50 to 100 mL/min. The initial stream of N_2 (100 ± 2 mL/min) was replaced by a N_2+CO_2 mixture (100 ± 2 mL/min); the precise N_2/CO_2 ratio is determined by the desired final CO_2 concentration, given that the total flow rate of the stream must be 100 ± 2 mL/min. After a flat characteristic plateau (equilibrium of partition coefficient) was attained, the chamber was flushed with pure N_2 to restore the starting conditions. Throughout the whole process, the coated quartz crystal frequency was measured as a function of the time every 1 s. All measurements were repeated at least four times, with variations in response less than 3%. The CO_2 vapor was supplied by SAPIO srl in gas cylinders with a certified concentration of 1000 ppm of CO_2 in nitrogen. The graduated cylinders were prepared following the standard gravimetric procedure of the normative ISO. For the high concentration measurements, we used a cylinder of pure CO_2.

■ ASSOCIATED CONTENT

Supporting Information. General experimental methods, reaction schemes for the synthesis of compounds **4**, **5**, and **8**, and NMR spectroscopic data (copies of 1D and 2D NMR spectra and tabular forms with assignments). This material is available free of charge via the Internet at http://pubs.acs.org.

■ AUTHOR INFORMATION

Corresponding Author
*E-mail: casnati@unipr.it.

■ ACKNOWLEDGMENT

We thank the Ministero dell'Istruzione, dell'Università e della Ricerca (MIUR, PRIN 2008 projects nos. 2008HZJW2L and 200858SA98) for the financial support and the Centro Interfacoltà di Misure (CIM) of the University of Parma for the use of NMR and mass spectrometers. We thank Dr. Davide Pedrini and Dr. Francesca Maffei for performing some QCM measurements. We also thank one of the referees for pointing out a misinterpretation of some DOSY data.

DEDICATION

§Dedicated to the memory of Dmitry M. Rudkevich, 1963−2007.

■ REFERENCES

(1) D'Alessandro, D.; Smit, B.; Long, J. *Angew. Chem., Int. Ed.* **2010**, *49*, 6058–6082.
(2) In H_2O, equilibria leading to the formation of carbonate and bicarbonate ions are also present.
(3) Dell'Amico, D. B.; Calderazzo, F.; Labella, L.; Marchetti, F.; Pampaloni, G. *Chem. Rev.* **2003**, *103*, 3857–3897.
(4) Song, J. H.; Yoon, J. H.; Lee, H.; Lee, K. H. *J. Chem. Eng. Data* **1996**, *41*, 497–499.
(5) Mandal, B. P.; Guha, M.; Biswas, A. K.; Bandyopadhyay, S. S. *Chem. Eng. Sci.* **2001**, *56*, 6217–6224.
(6) Aresta, M.; Quaranta, E. *Tetrahedron* **1992**, *48*, 1515–1530.
(7) McGhee, W.; Riley, D.; Christ, K.; Pan, Y.; Parnas, B. *J. Org. Chem.* **1995**, *60*, 2820–2830.
(8) Arakawa, H.; Aresta, M.; Armor, J. N.; Barteau, M. A.; Beckman, E. J.; Bell, A. T.; Bercaw, J. E.; Creutz, C.; Dinjus, E.; Dixon, D. A.; Domen, K.; DuBois, D. L.; Eckert, J.; Fujita, E.; Gibson, D. H.; Goddard, W. A.; Goodman, D. W.; Keller, J.; Kubas, G. J.; Kung, H. H.; Lyons, J. E.; Manzer, L. E.; Marks, T. J.; Morokuma, K.; Nicholas, K. M.; Periana, R.; Que, L.; Rostrup-Nielson, J.; Sachtler, W. M. H.; Schmidt, L. D.; Sen, A.; Somorjai, G. A.; Stair, P. C.; Stults, B. R.; Tumas, W. *Chem. Rev.* **2001**, *101*, 953–996.
(9) Salvatore, R. N.; Shin, S. I.; Nagle, A. S.; Jung, K. W. *J. Org. Chem.* **2001**, *66*, 1035–1037.
(10) Ion, A.; Van Doorslaer, C.; Parvulescu, V.; Jacobs, P.; De Vos, D. *Green Chem.* **2008**, *10*, 111–116.
(11) Zhou, R.; Vaihinger, S.; Geckeler, K. E.; Göpel, W. *Sens. Actuators, B* **1994**, *19*, 415–420.
(12) Brousseau, L. C.; Aurentz, D. J.; Benesi, A. J.; Mallouk, T. E. *Anal. Chem.* **1997**, *69*, 688–694.
(13) Herman, P.; Murtaza, Z.; Lakowicz, J. R. *Anal. Biochem.* **1999**, *272*, 87–93.
(14) Hampe, E. M.; Rudkevich, D. M. *Tetrahedron* **2003**, *59*, 9619–9625.

(15) Alauzun, J.; Besson, E.; Mehdi, A.; Reyé, C.; Corriu, R. J. P. *Chem. Mater.* **2008**, *20*, 503–513.
(16) George, M.; Weiss, R. G. *J. Am. Chem. Soc.* **2001**, *123*, 10393–10394.
(17) George, M.; Weiss, R. G. *Langmuir* **2002**, *18*, 7124–7135.
(18) Leclaire, J.; Husson, G.; Devaux, N.; Delorme, V.; Charles, L.; Ziarelli, F.; Desbois, P.; Chaumonnot, A.; Jacquin, M.; Fotiadu, F. D. R.; Buono, G. R. *J. Am. Chem. Soc.* **2010**, *132*, 3582–3593.
(19) Carretti, E.; Dei, L.; Baglioni, P.; Weiss, R. G. *J. Am. Chem. Soc.* **2003**, *125*, 5121–5129.
(20) Stastny, V.; Anderson, A.; Rudkevich, D. M. *J. Org. Chem.* **2006**, *71*, 8696–8705.
(21) Stastny, V.; Rudkevich, D. M. *J. Am. Chem. Soc.* **2007**, *129*, 1018–1019.
(22) Xu, H.; Rudkevich, D. M. *Chem.—Eur. J.* **2004**, *10*, 5432–5442.
(23) Xu, H.; Rudkevich, D. M. *Org. Lett.* **2005**, *7*, 3223–3226.
(24) Zhang, H.; Rudkevich, D. M. *Chem. Commun.* **2007**, 4893–4894.
(25) Dibenedetto, A.; Aresta, M.; Fragale, C.; Narracci, M. *Green Chem.* **2002**, *4*, 439–443.
(26) Baldini, L.; Casnati, A.; Sansone, F.; Ungaro, R. *Chem. Soc. Rev.* **2007**, *36*, 254–266.
(27) At concentration higher than 0.01 M, compound **1** is scarcely soluble in $CDCl_3$.
(28) Masuda, K.; Ito, Y.; Horiguchi, M.; Fujita, H. *Tetrahedron* **2005**, *61*, 213–229.
(29) Cohen, Y.; Avram, L.; Frish, L. *Angew. Chem., Int. Ed.* **2005**, *44*, 520–554.
(30) Where k is the Boltzmann constant and T is the absolute temperature.
(31) Macchioni, A.; Ciancaleoni, G.; Zuccaccia, C.; Zuccaccia, D. *Chem. Soc. Rev.* **2008**, *37*, 479–489.
(32) Ikeda, A.; Tsuzuki, H.; Shinkai, S. *J. Chem. Soc., Perkin Trans. 2* **1994**, 2073–2080.
(33) Arduini, A.; Fabbi, M.; Mantovani, M.; Mirone, L.; Pochini, A.; Secchi, A.; Ungaro, R. *J. Org. Chem.* **1995**, *60*, 1454–1457.
(34) George, M.; Weiss, R. G. *Langmuir* **2003**, *19*, 8168–8176.
(35) Dalcanale, E.; Hartmann, J. *Sens. Actuators, B* **1995**, *24*, 39–42.
(36) Tonezzer, M.; Melegari, M.; Maggioni, G.; Milan, R.; Mea, G. D.; Dalcanale, E. *Chem. Mater.* **2008**, *20*, 6535–6542.
(37) A control experiment with 1-adamanthylamine led to negligible responses under the same conditions of coating and CO_2 exposure.
(38) In order to obtain Δf values comparable to those produced by layer **4** upon exposure to 20 ppm of CO_2, layer **8** was exposed to a 10 times larger CO_2 concentration.
(39) Elovich, S. Yu.; Zhabrova, G. M. *Zh. Fiz. Khim.* **1939**, *13*, 1761–1774.
(40) Dooling, C. M.; Worsfold, O.; Richardson, T. H.; Tregonning, R.; Vysotsky, M. O.; Hunter, C. A.; Kato, K.; Shinbo, K.; Kaneko, F. *J. Mater. Chem.* **2001**, *11*, 392–398.
(41) Arnold, D. P.; Manno, D.; Micocci, G.; Serra, A.; Tepore, A.; Valli, L. *Langmuir* **1997**, *13*, 5951–5956.
(42) Okunola, O. A.; Seganish, J. L.; Salimian, K. J.; Zavalij, P. Y.; Davis, J. T. *Tetrahedron* **2007**, *63*, 10743–10750.
(43) Oprea, A.; Henkel, K.; Oehmgen, R.; Appel, G.; Schmeisser, D.; Lauer, H.; Hausmann, P. *Mater. Sci. Eng., C* **1999**, *8−9*, 509–512.
(44) Zhou, R.; Schmeisser, D.; Gopel, W. *Sens. Actuators, B* **1996**, *33*, 188–193.
(45) Casnati, A.; Della Ca', N.; Fontanella, M.; Sansone, F.; Ugozzoli, F.; Ungaro, R.; Liger, K.; Dozol, J. F. *Eur. J. Org. Chem.* **2005**, 2338–2348.
(46) Barboso, S.; Carrera, A. G.; Matthews, S. E.; Arnaud-Neu, F.; Böhmer, V.; Dozol, J. F.; Rouquette, H.; Schwing-Weill, M. J. *J. Chem. Soc., Perkin Trans. 2* **1999**, 719–723.
(47) Bagnacani, V.; Sansone, F.; Donofrio, G.; Baldini, L.; Casnati, A.; Ungaro, R. *Org. Lett.* **2008**, *10*, 3953–3956.
(48) Casnati, A.; Fochi, M.; Minari, P.; Pochini, A.; Reggiani, M.; Ungaro, R.; Reinhoudt, D. N. *Gazz. Chim. Ital.* **1996**, *126*, 99–106.
(49) Dondoni, A.; Marra, A.; Scherrmann, M. C.; Casnati, A.; Sansone, F.; Ungaro, R. *Chem.—Eur. J.* **1997**, *3*, 1774–1782.
(50) Casnati, A.; Pochini, A.; Ungaro, R.; Ugozzoli, F.; Arnaud, F.; Fanni, S.; Schwing, M. J.; Egberink, R. J. M.; de Jong, F.; Reinhoudt, D. N. *J. Am. Chem. Soc.* **1995**, *117*, 2767–2777.
(51) Dondoni, A.; Ghiglione, C.; Marra, A.; Scoponi, M. *J. Org. Chem.* **1998**, *63*, 9535–9539.
(52) SPARTAN 10, Release 1.0.1, Wavefunction, Inc., Irvine, CA 92612, http://www.wavefun.com, 2010.
(53) Ballatine, D. S.; White, R. M.; Martin, S. J.; Ricco, A. J.; Zellers, E. T.; Frye, G. C.; Wihltjen, H., Eds. *Acoustic Wave Sensors*; Academic Press: San Diego, CA, 1997.
(54) Ozturk, Z. Z.; Zhou, R.; Weimar, U.; Ahsen, V.; Bekaroglu, O.; Gopel, W. *Sens. Actuators, B* **1995**, *26*, 208–212.